INVESTIGATION OF JET NOISE CHARACTERISTICS FROM A GAS TURBINE NOZZLE USING AN INTEGRATED CFD - CAA APPROACH CONSIDERING FLOW VELOCITY EFFECTS

Thanh Dong Pham[1,*], Van Quang Ngo[2], Ba Van Le[3], Ngoc Thanh Dang[1]

[1]*Faculty of Aerospace Engineering, Le Quy Don Technical University*

[2]*Faculty of Systems Engineering, Le Quy Don Technical University*

[3]*Faculty of Aeronautical Engineering, Air Defense - Air Force Academy*

Abstract

This article presents an integrated Computational Fluid Dynamics - Computational Aeroacoustics (CFD-CAA) approach for investigating jet noise characteristics generated by a gas turbine engine nozzle under subsonic conditions. The aerodynamic field is simulated using the Unsteady Reynolds-Averaged Navier-Stokes (URANS) method with the k–ω SST turbulence model to obtain the unsteady velocity field, combined with the Broadband Noise Model in Ansys Fluent to predict the Acoustic Power Level (APL). The research object is the NASA acoustic reference nozzle (ARN2). The model was validated through comparison of the velocity field with published PIV data. After validation, parametric studies are conducted to assess the influence of the freestream Mach number and jet Mach number on the acoustic power level. Results indicate that APL increases marginally with the freestream Mach number (approximately 2.2%), but increases significantly with the jet Mach number (a 10.3% increase when Mjet increases from 0.513 to 0.75). The URANS-Broadband approach demonstrates acceptable reliability in analyzing noise variation trends while significantly reducing computational costs compared to several other methods.

Keywords: *Broadband noise; CFD-CAA; ARN nozzle; jet noise; URANS.*

1. Introduction

Jet noise is the primary noise source of jet engines and subsonic rockets, generated by turbulent interactions between the core flow and the surrounding environment according to Lighthill's acoustic analogy mechanism [1]. The main components include: total jet noise, shock-associated noise (in supersonic flows), and interaction noise.

Current research on jet aeroacoustics has increasingly relied on high-fidelity approaches such as Large Eddy Simulation (LES) and hybrid RANS/LES methods to resolve turbulent structures responsible for acoustic radiation [2], [3]. NASA's studies on

* Corresponding author, email: pham.thanh-dong@lqdtu.edu.vn
DOI:

the PIV dataset for the Acoustic Reference Nozzles (ARN) have established a reliable benchmark foundation for numerical models [4], [5]. Besides, the field of Computational Aeroacoustics (CAA) has achieved significant progress in modeling nonlinear acoustic sources and noise generation mechanisms from turbulent flows [6]. In addition, acoustic analogy methods, typically the Ffowcs Williams–Hawkings method, continue to be improved to enhance the accuracy in predicting the acoustic field in the time domain [7]. The trend of using hybrid methods between LES and acoustic models like FWH is also widely applied to predict jet noise with higher accuracy in both the near and far fields [8].

However, LES methods require massive computational resources (around 10^8 mesh cells), making them difficult to deploy widely in laboratory conditions lacking powerful server systems. Therefore, an intermediate approach with acceptable accuracy, along with low time and resource costs, is a necessary direction to perform a series of noise problems in the preliminary calculation phase, serving the investigation and directional research process.

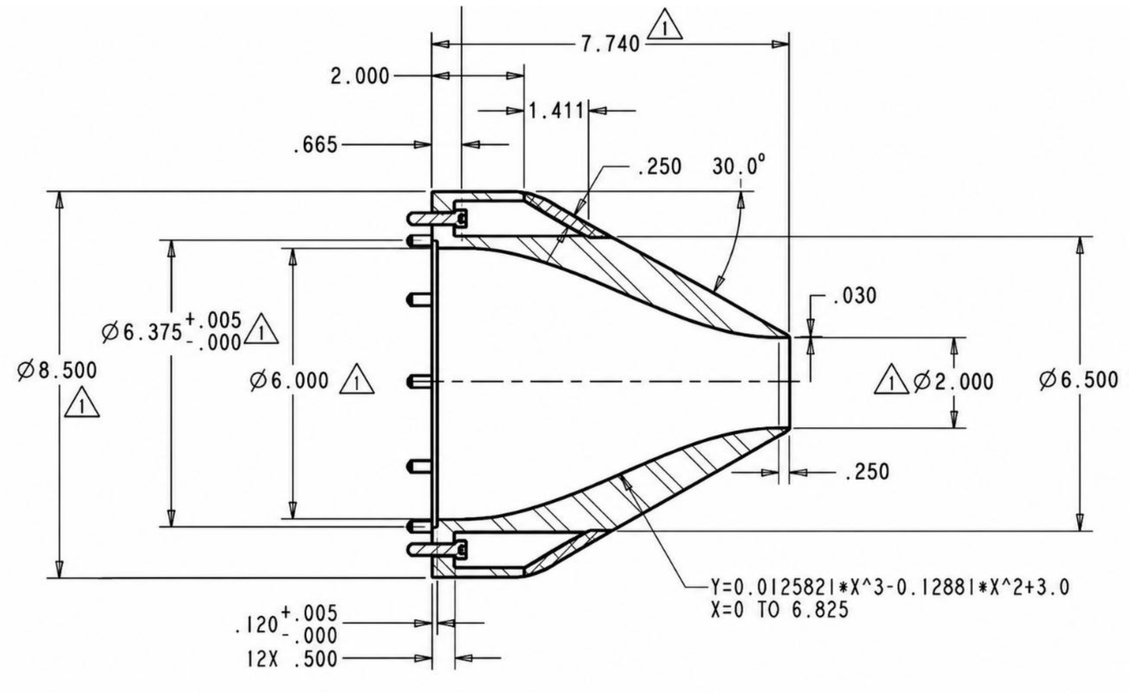

Fig. 1. Geometric dimensions of the nozzle model (ARN2) [4].

In this article, the authors focus on establishing an integrated URANS - Broadband model, validated by NASA data, to evaluate the trend of noise variation according to freestream and jet velocities with significantly lower time and computational resource costs compared to LES.

2. Simulation method

2.1. Nozzle model

The research object is the ARN2 acoustic reference nozzle developed by NASA [4], with an exit diameter of $D_{jet} = 50.8\ mm$, and specific geometric dimensions shown in Fig. 1. The model is built in 3D using Ansys DesignModeler [9] (Fig. 2) and exploits the axisymmetric nature of the nozzle to reduce the computational domain (Fig. 3).

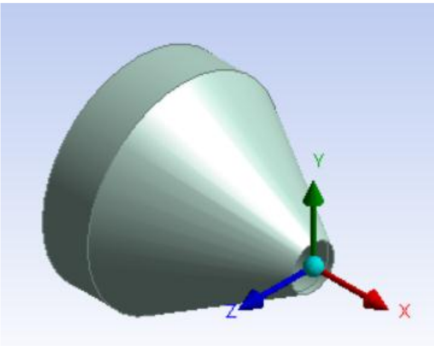

Fig. 2. 3D model of the ARN2 nozzle.

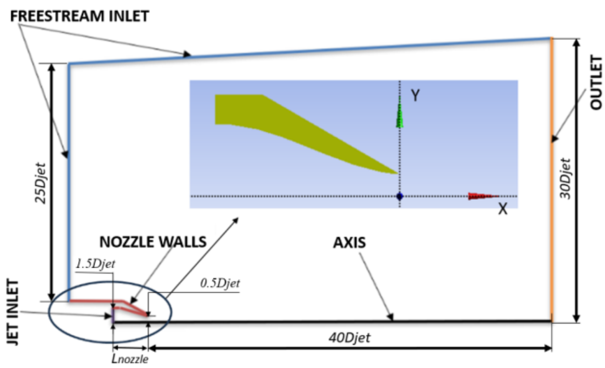

Fig. 3. Simulation domain and boundary conditions.

2.2. Simulation domain and meshing

Given that the geometric structure of the ARN2 nozzle is fully axisymmetric, and the Broadband Noise acoustic method used in the study relies on time-averaged turbulence quantities (turbulent kinetic energy k and dissipation rate ω) extracted from URANS to predict the interpolated noise source, it does not require directly solving the 3D acoustic wave propagation like FWH or LES. Therefore, the axisymmetric flow field in the 2D model is sufficiently reliable to provide input for the acoustic model, while meeting the objective of reducing computational costs aimed at by the article. Thus, the simulated computational domain (shown in Fig. 3) is established with the main components and boundary conditions as follows (Tab. 1):

Tab. 1. Simulation setup parameters

Boundary condition	**Value**	**Setup parameters**	**Value**
Freestream inlet	Pressure far-field	Time step size, s	0.0001
Jet inlet	Pressure inlet	Number of iterations/time step	20
Outlet	Pressure outlet	Number of time steps	1000
Nozzle walls	Wall no-slip	Model convergence iterations	17500
Axis	Symmetry	Turbulence model	*k-ω SST*

The structured mesh is refined at the nozzle lip and the shear layer region (Fig. 4(a)). A grid convergence study was performed with 3 resolution levels: coarse (mesh1), medium (mesh2), and fine (mesh3), corresponding to 118,500, 190,000, and 280,000 elements, respectively. The computational mesh was selected based on the balance between the convergence of the axial flow velocity compared to NASA's experimental data and the computational time. The distribution of the axial flow velocity according to the grid resolution levels (coarse, medium, fine) is presented in Fig. 4(b).

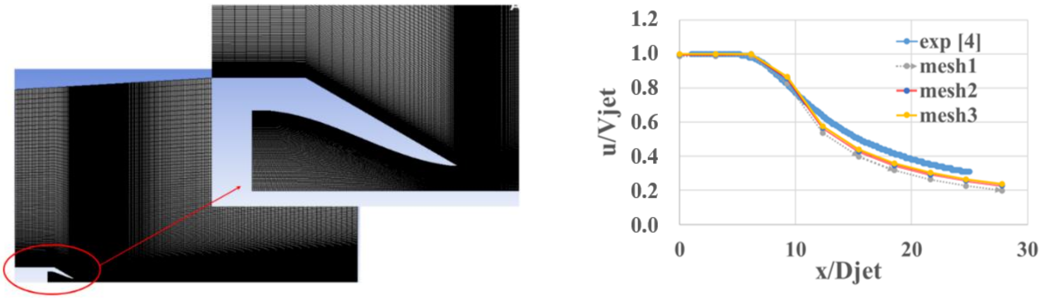

a) Structured mesh *b) Mesh convergence*

Fig. 4. Structured mesh and mesh convergence.

It can be observed in Fig. 4(b) that all three mesh levels (mesh1, mesh2, mesh3) reproduce the general physical trend of the jet flow, with the axial velocity remaining almost constant in the region near the nozzle exit and gradually decreasing with distance due to the turbulent mixing process. However, the difference between the grids is evident in the accuracy of the axial velocity component values as well as the degree of agreement with the experimental data. Specifically, mesh1 (coarse mesh) tends to predict lower velocities compared to the experiment in the far region. This is a consequence of large numerical diffusion, leading to a faster-than-actual momentum decay and distorting the flow characteristics. Conversely, mesh3 (fine mesh) yields results very close to mesh2 and slightly improved over mesh1; however, the improvement level compared to mesh2 is insignificant. The difference between mesh2 and mesh3 across the entire computational domain is very small, especially in the flow development region, indicating that the solution has approached a grid-independent state.

Notably, mesh2 represents an optimal balance between accuracy and computational cost. Results from mesh2 follow the experimental data better than mesh1 and almost coincide with mesh3, proving that the main characteristics of the flow have been fully described. Meanwhile, the use of mesh3 only significantly increases the number of elements and calculation time without bringing a proportional improvement in accuracy. Therefore, it can be concluded that mesh2 is a reasonable choice, as it ensures the reliability of the simulation results while optimizing computational resources. This also aligns with the general principle in numerical research: a grid is selected when the solution reaches a nearly unchanging state upon further grid refinement.

2.3. Aerodynamic model

The Density-Based, implicit solver was used with an ideal gas, $\gamma = 1.4$. The chosen turbulence model is *k-ω SST* with a convergence criterion of 10^{-4}.

The relationship between total pressure and Mach number:

$$\frac{p_t}{p_{ref}} = \left(1 + \frac{\gamma - 1}{2} M_{jet}^2\right)^{\frac{\gamma}{\gamma - 1}}$$

where p_t is total pressure at the nozzle inlet; p_{ref} is reference pressure, $p_{ref} = 101325$ Pa; M_{ref} is reference Mach number; M_{jet} is Mach number at the nozzle exit; γ is specific heat ratio of the gas, $\gamma = 1.4$.

2.4. Acoustic model

The Broadband Noise Model in Ansys Fluent is used, suitable for rapid assessment of near-field APL (Acoustic Power Level) (Fig. 5). Compared to FWH, the Broadband Noise model does not require saving large unsteady fields, which is suitable for parametric trend studies and reduces storage costs. The Broadband Noise model is used in the article to directly evaluate the Acoustic Source Power or Acoustic Power Level (APL) generated from turbulent fluctuations in the near-field right inside the computational domain, without the need to determine discrete receiver points in the far-field, as in the approach of solving the Ffowcs Williams-Hawkings (FWH) acoustic wave propagation equation.

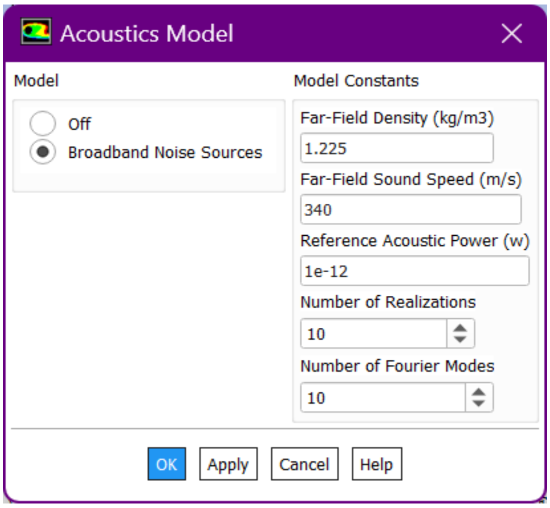

Fig. 5. Acoustic model in Ansys Fluent.

3. Results and discussion

3.1. Velocity field validation

The calculated velocity results on the investigated lines in the article are compared with NASA's PIV dataset [4]. The straight line line1 – along the *x*-direction, starts from the origin and has a length of 28*Djet*; line2, line5, line10, line15, line20 all have a length of 1.5*Djet* – along the *Y*-axis and perpendicular to the *X*-axis at $x = 2Djet$, $x = 5Djet$, $x = 10Djet$, $x = 15Djet$, $x = 20Djet$, respectively (Figs. 6, 7). The flow velocity magnitude is concentrated at the center and gradually decreases towards the two boundaries. The flow velocity at any point in the simulation region has two components (*u*, *v*), where *u* is the axial component in the X direction, and v is the radial component in the Y direction. The *XOY* coordinate system and the investigation lines are arranged as shown in Fig. 6.

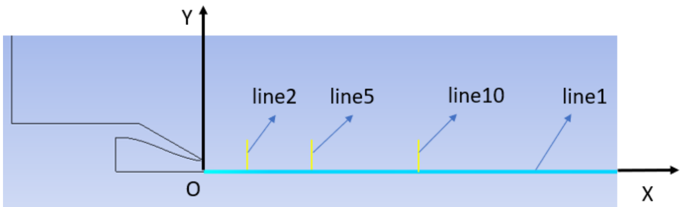

Fig. 6. Position of data extraction lines.

Under the simulation conditions, Freestream inlet: Pressure far field, $M_{ref} = 0.01$; Jet inlet: Pressure-inlet, $p_t/p_{ref} = 1.19671$. Observing the simulated image of the axial velocity u of the flow after the nozzle in Fig. 7 shows that the simulation model of the article yields relatively similar results in color distribution, value, and flow structure.

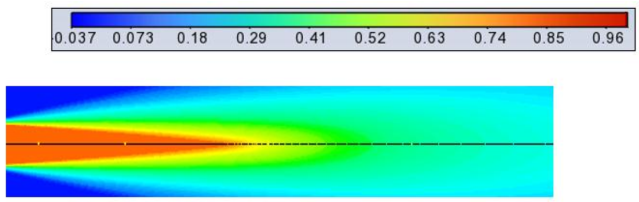

a) Flow velocity simulation image from the paper

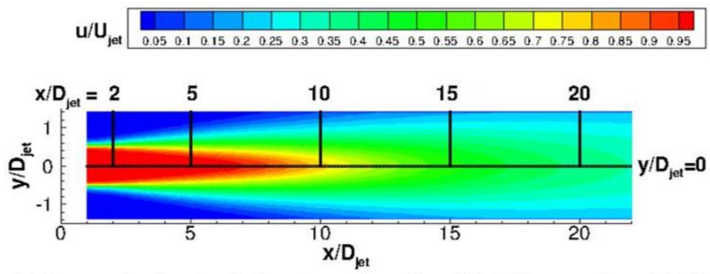

b) Flow velocity simulation image based on NASA's experimental PIV data [4]

Fig. 7. Simulation of the axial flow velocity.

Although the velocity component *v* of the jet flow downstream of the nozzle does not hold a large value in the total flow velocity, it represents a dispersive significance. The calculated and experimental values of the velocity component v on the straight lines line2, line5, line10, line15, line20 are presented in Fig. 8.

The maximum value deviation is < 5%, proving that the calculation results from the URANS model in this article are sufficiently reliable to be used as input for acoustic calculations. Thus, it can be seen that although URANS does not explicitly resolve large coherent turbulent structures like LES, it accurately reproduces the mean velocity distribution - the dominant factor for broadband acoustic source energy in the subsonic regime.

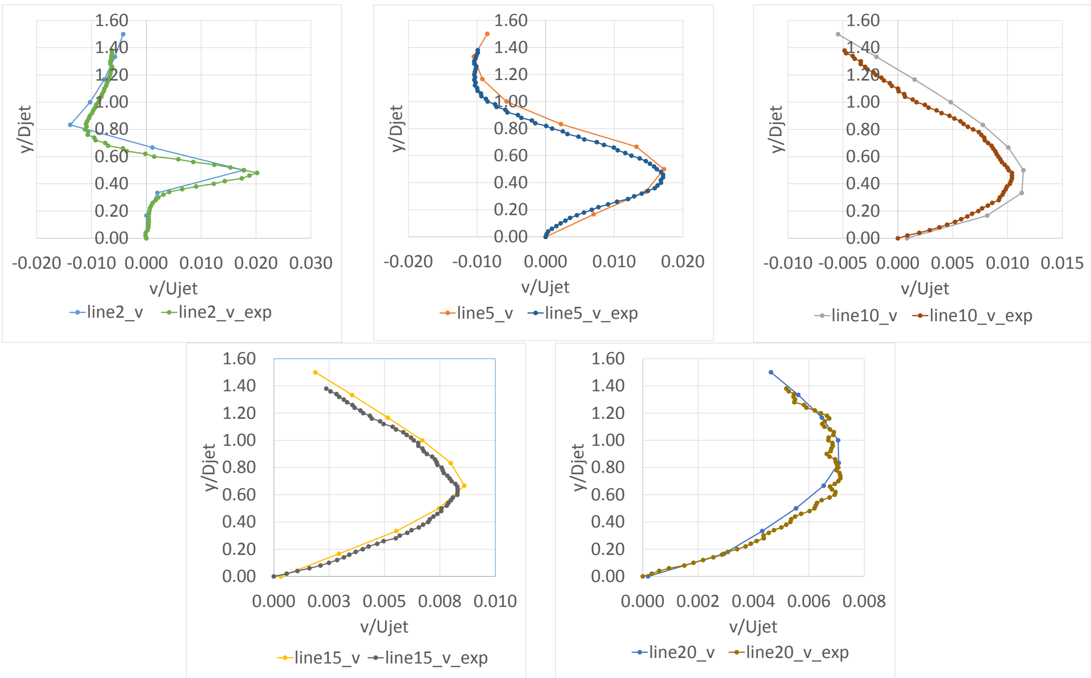

Fig. 8. Velocity component v of the jet flow.

Through the calculation results, it can be seen that compared to high-fidelity simulation methods like LES or hybrid RANS/LES presented in studies, the URANS method has certain limitations but offers an outstanding advantage in cost. Specifically, regarding the ability to reproduce the flow and acoustic fields, LES can directly resolve large vortex structures, allowing detailed prediction of far-field noise frequency spectra. Meanwhile, URANS combined with Broadband only calculates the time-averaged flow field and predicts the acoustic power level (APL) based on turbulent quantities (k, ω), leading to a maximum deviation in the transverse velocity component of below 5%

compared to experimental PIV. However, in terms of computational cost, LES simulation for the jet noise problem often requires a computational grid of hundreds of millions of elements (about 10^8 mesh cells) and thousands of CPU hours on a high-performance server system. Conversely, the URANS-Broadband method, as in this study, does not require a massive number of grid elements and can be completed on a standard workstation in a short time. This demonstrates that the URANS - Broadband approach is an effective intermediate tool, balancing between accuracy (well reproducing the V^8 scaling law) and computational cost, making it particularly suitable for preliminary design steps.

3.2. Effect of freestream Mach number (M_{ref})

Varying the M_{ref} values in the range of 0.01–0.2, we obtain the calculated results for the maximum acoustic power level in each case as shown in Tab. 2. The simulated image of the acoustic power level parameter at the condition M_{ref} = 0.01 is shown in Fig. 9. APL reaches a maximum value of 137.37 dB right at the nozzle exit lip, closely following the outer boundary of the nozzle wall. This is the region where the gas flow is strongly compressed, creating the maximum acoustic power level. Conversely, in the core region of the nozzle, where the flow velocity reaches its highest value, the flow is not compressed, and the noise value is not high. At a distance of about $8D_{jet}$ from the nozzle exit, the compressed flows at both sides of the nozzle exit lip interfere and create a spatial region downstream of the nozzle with high noise values (about 90–125 dB). The high-value noise region continues to expand to a distance of $18D_{jet}$ before gradually decreasing. The acoustic power level drops to a low average value (about 55–65 dB).

Tab. 2. Maximum acoustic power level of the jet flow at different M_{ref} values

M_{ref}	0.01	0.02	0.05	0.1	0.2
APLmax (dB)	137.37	137.81	138.37	139.12	140.27

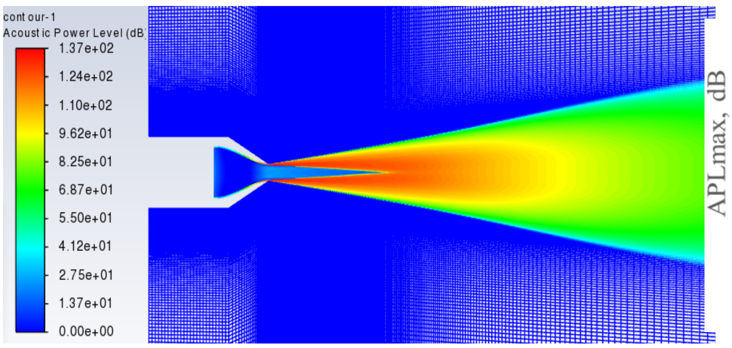

Fig. 9. Contours of acoustic power level (APL) at M_{ref} = 0.01.

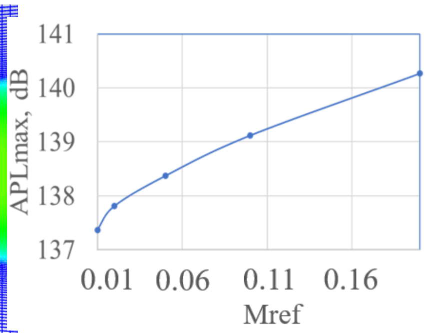

Fig. 10. Variation of APLmax with M_{ref}.

From the data in Tab. 2, Fig. 10 presents a graph showing the variation of *APLmax* (dB) according to the freestream Mach number M_{ref}. The graph shows that the maximum acoustic power level of the jet flow gradually increases with the increase in the freestream Mach number; however, the increase in APLmax is not overly large (at most only 2.2% at M_{ref} = 0.2 – when the freestream Mach number increases 20 times). Freestream flow reduces the velocity gradient at the shear layer between the jet flow and the environment, thereby slightly reducing the turbulence generation intensity. However, the main energy source generating noise still comes from the kinetic energy of the jet core (according to Lighthill's acoustic analogy theory), so varying M_{ref} in the low-velocity range brings a very small noise variation effect.

3.3. Effect of jet Mach number (M_{jet})

Varying the jet exit Mach number M_{jet} according to the range of values in Table 3 to study the effect of the jet velocity at the nozzle exit on the noise characteristics generated by the flow.

Tab. 3. Maximum acoustic power level of the jet flow at different Mjet values

M_{jet}	0.513	0.55	0.6	0.65	0.7	0.75
APLmax (dB)	137.37	140	143	146	149	151.5

The maximum acoustic power level APLmax in Tab. 3 gradually increases with the increase of M_{jet} and reaches the highest value of 151.5 dB at M_{jet} = 0.75, an increase of 14.13 dB (a 10.3% increase when M_{jet} increases 1.46 times). This is consistent with the empirical law: $APL \sim U^n$, where $n \approx 7–8$ (Fig. 11) for subsonic flows presented in [1], [3], [5].

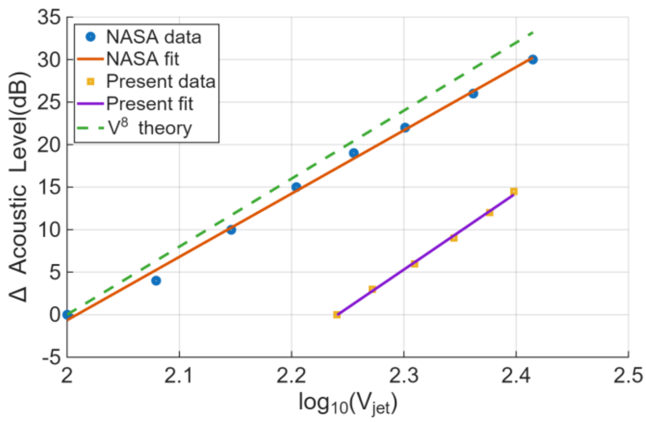

Fig. 11. Relative acoustic variation (ΔOASPL/ΔAPLmax) according to Mach number.

The maximum acoustic power level values (shown in Tab. 2, Tab. 3, and Fig. 9) are extracted directly from the spatial region of the shear layer located right after the nozzle exit lip, extending from the position $0D_{jet}$ to $18D_{jet}$ along the flow axis, where the turbulent energy and flow compression reach their highest values.

In NASA reports, the SHJAR system uses an array of 24 microphones placed on a circular arc with a radius of 100 inches (about 2.54 meters). At this distance (equivalent to about 50 times the diameter of the ARN2 nozzle), the microphones are located in the far-field region. The value measured by NASA at these microphones is the Sound Pressure Level (SPL) of the acoustic waves after propagating through the air from the jet flow to the microphone diaphragms. Broadband models (as in this article) do not solve the acoustic wave propagation equation. They use turbulent quantities (k, ω) from the URANS model to calculate the Acoustic Power Level (APL) generated right at the grid nodes inside the turbulent flow (near field).

Therefore, it is impossible to directly compare the acoustic source power level (radiated at the flow core) with the sound pressure level (measured at a distance of 2.54 meters). However, it is possible to validate the acoustic calculation results in the article using the variation law. According to Lighthill's theory and NASA data, the total acoustic energy radiated from the jet flow (Acoustic Power – determined from Broadband models as in this study) and the sound pressure in the far-field (OASPL – measured by NASA) both follow the same proportion, which is the 8th power of the jet flow velocity (V_{jet}^{8}). The relative increase/decrease of the data in reference (ΔOASPL) and of the data in this article (ΔAPLmax) are represented in Fig. 11.

The comparison in Fig. 11 shows that the variation trend of the simulated acoustic power level agrees well with both the far-field OASPL data reported by NASA and the theoretical (V^8) scaling law proposed by Lighthill. Although the Broadband model predicts near-field acoustic source power while NASA measurements represent far-field sound pressure, both quantities exhibit a consistent dependence on jet velocity. This agreement in slope indicates that the present URANS–Broadband model captures the dominant jet-noise generation mechanism. Differences in absolute magnitude between APL and OASPL are expected because they correspond to different physical quantities and are affected by propagation distance, radiation direction, and measurement conditions. Therefore, in the present study, agreement in variation trend rather than direct magnitude matching is adopted as the primary validation criterion. This supports the suitability of the proposed approach for predicting near-field jet-noise trends with reduced computational cost.

4. Conclusion

The article has successfully applied an integrated CFD-CAA model with URANS and Broadband to calculate and simulate jet noise from a gas turbine engine nozzle. The model is validated for accuracy and reliability using PIV data published by NASA. Quantitative results show that APLmax increases exponentially with respect to the jet flow velocity, increasing by 14.13 dB corresponding to 10.3% when M_{jet} increases 1.46 times, well reproducing Lighthill's V^8 law, while the freestream Mach number variation only changes the maximum noise amplitude by 2.2% when M_{ref} increases 20 times.

The proposed method in the article is suitable for preliminary optimization research and parametric trend evaluation under limited computational resources. In future developments, it will study the combination with the FWH model to analyze frequency spectra or use ZDES/IDDES simulation methods to increase the accuracy of calculated data. Future work will extend the present framework to FWH-based spectral prediction and optimized chevron-nozzle configurations.

Acknowledgment

This research is funded by Le Quy Don Technical University Research Fund under the under the grant number 25.01.30.

References

[1] M. J. Lighthill, "On sound generated aerodynamically I. General theory", in *Proceedings of the Royal Society of London. Series A. Mathematical and Physical Sciences*, 211.1107, pp. 564–587, 1952. DOI: 10.1098/rspa.1952.0060

[2] D. J. Bodony and S. K. Lele, "Current status of jet noise predictions using large-eddy simulation", *AIAA Journal*, Vol. 46, No. 2, pp. 364–380, 2008. DOI: 10.2514/1.24475

[3] G. A. Brès, F. E. Ham, J. W. Nichols, and S. K. Lele, "Unstructured large-eddy simulations of supersonic jets", *AIAA Journal*, Vol. 55, Iss. 4, pp. 1164–1184, 2017. DOI: 10.2514/1.J055084

[4] J. Bridges and M. P. Wernet, "The NASA subsonic jet particle image velocimetry (PIV) dataset", No. E-17439, 2011.

[5] C. Brown and J. Bridges, *Small Hot Jet Acoustic Rig Validation*, No. E-15481, 2006. [Online]. Available: https://ntrs.nasa.gov/api/citations/20060013451/downloads/20060013451.pdf

[6] Y. Zhang, Y. Xiao, H. Chen, and R. Liu, "Aeroacoustic prediction based on large-eddy simulation and the Ffowcs Williams – Hawkings equation", *Advances in Aerodynamics*, Vol. 4, No. 1, 2022. DOI: 10.1186/s42774-022-00112-2

[7] ANSYS Inc., *ANSYS Fluent Theory Guide*, Release 2021 R1, 2021

[8] D. Casalino, "An advanced time approach for acoustic analogy predictions", *Journal of Sound and Vibration*, Vol. 261, No. 4, pp. 583–612, 2003. DOI: 10.1016/S0022-460X(02)00986-0.

[9] T. Colonius and S. K. Lele, "Computational aeroacoustics: progress on nonlinear problems of sound generation", *Progress in Aerospace Sciences*, Vol. 40, Iss. 6, pp. 345–416, 2004. DOI: 10.1016/j.paerosci.2004.09.001

NGHIÊN CỨU ĐẶC TRƯNG TIẾNG ỒN DÒNG PHẢN LỰC TỪ LOA PHỤT ĐỘNG CƠ TUA BIN KHÍ BẰNG MÔ HÌNH TÍCH HỢP CFD - CAA XÉT ĐẾN ẢNH HƯỞNG CỦA TỐC ĐỘ DÒNG

Phạm Thành Đồng[1], Ngô Văn Quảng[2], Lê Bá Vân[3], Đặng Ngọc Thanh[1]

[1]*Khoa Hàng không vũ trụ, Trường Đại học Kỹ thuật Lê Quý Đôn*

[2]*Khoa Kỹ thuật hệ thống, Trường Đại học Kỹ thuật Lê Quý Đôn*

[3]*Khoa Kỹ thuật hàng không, Học viện Phòng không – Không quân*

Tóm tắt: Bài báo trình bày phương pháp mô phỏng tích hợp CFD - CAA nhằm nghiên cứu đặc trưng tiếng ồn của dòng phản lực từ loa phụt động cơ tua bin khí trong điều kiện cận âm. Mô hình khí động sử dụng URANS với mô hình chảy rối *k–ω* SST để thu trường vận tốc không dừng, kết hợp mô hình Broadband Noise trong Ansys Fluent để dự đoán mức công suất nguồn âm (APL). Đối tượng nghiên cứu là loa phụt chuẩn âm học ARN2 của NASA. Mô hình được kiểm chứng thông qua đối sánh trường vận tốc với dữ liệu thực nghiệm PIV đã công bố. Sau kiểm chứng, thực hiện nghiên cứu khảo sát ảnh hưởng của số Mach của dòng bao ngoài và dòng phản lực đến mức công suất nguồn âm. Kết quả cho thấy APL tăng không đáng kể theo số Mach của dòng bao ngoài (≈ 2,2%), nhưng tăng mạnh theo số Mach của dòng phản lực (tăng 10,3% khi M_{jet} tăng từ 0,513 lên 0,75). Cách tiếp cận URANS-Broadband cho thấy độ tin cậy chấp nhận được trong phân tích xu hướng biến thiên tiếng ồn, đồng thời giảm đáng kể chi phí tính toán so với một số phương pháp khác.

Từ khóa: *Tiếng ồn dải rộng; CFD-CAA; loa phụt ARN; tiếng ồn phản lực; URANS.*

Received: 05/03/2026; Revised: 15/05/2026; Accepted for publication: …/05/2026

❑